Journal of Catalysis **201,** 198–205 (2001)
doi:10.1006/jcat.2001.3252, available online at http://www.idealibrary.com on IDEAL®

H_2O Splitting in Tubular PACT (Plasma and Catalyst Integrated Technologies) Reactors

Xiao Chen,* Steven L. Suib,*,†,‡,[1] Yuji Hayashi,§ and Hiroshige Matsumoto¶

*Department of Chemistry, †Department of Chemical Engineering, and ‡Institute of Material Science, University of Connecticut, Storrs, Connecticut 06269; §Fujitsu Laboratories, Ltd., 1015 Kamikodanaka, Nakahara, 211 Japan; and ¶Department of Chemistry, Nagasaki University, Bunkyomachi 1-14, Nagasaki, 852 Japan

Received October 24, 2000; revised April 19, 2001; accepted April 27, 2001

Significant hydrogen production (0.33 mol% in products) from H_2O splitting by atmospheric dielectric barrier discharges has been achieved with tubular PACT reactors at room temperature. Effects of different experimental parameters, such as different metal (either Ni, Pd, Rh, or Au) coated inner electrodes, types and lengths of outer metal (either Al or Cu) electrodes, grounding states of the inner and outer electrodes, AC peak voltages applied on the reactor, and the flow rate of the feed (2.3 mol% in Ar), have been systematically studied. The water splitting activity varies when the type of metal-coated inner electrodes, peak voltage, the length of outer electrode, and the flow rate of the feed change, but does not depend on the types of outer metal electrodes and the grounding states of the inner and outer electrodes. © 2001 Academic Press

1. INTRODUCTION

The unevenly distributed and limited world fossil fuel reserves are predicted to be exhausted in the middle of the twenty-first century (1). Recently, the concern over the environmental pollution by the usage of fossil fuels, particularly by automobiles, has been growing vigorously. All of these have driven various studies to search for alternative cleaner energy sources. Hydrogen, as an energy carrier, is one of the most favorable alternative energy sources because it is a clean, renewable, and nonpolluting fuel.

Presently, most of the world's hydrogen is produced via catalytic steam reforming of hydrocarbon sources, such as coal, oil, or natural gas. To eliminate the reliance on fossil fuels, an alternative source of hydrogen must be found. The unlimited water source appears to be the most appealing for extracting large amounts of hydrogen for widespread energy use. Many processes have been proposed to exploit this abundant source of hydrogen; all of them involve the splitting of water into hydrogen and oxygen.

Czuppon *et al.* (2) presented an excellent review on different water-splitting techniques, such as, one-step thermal or multistep thermochemical water splitting, water splitting by solar energy, and electrochemical water splitting (electrolysis). One-step thermal water splitting requires very high temperatures, usually higher than 2000°C. The devices that can withstand such high temperatures are presently both inefficient and uneconomical. More practical interest has been focused on multistep water splitting processes, which generally involve multistep thermochemical reactions and/or electrolysis steps. These thermochemical reactions are thermally conducted at temperatures much lower than those for one-step thermal water splitting, and electrolysis steps are driven at voltages lower than those used in conventional water electrolysis in order to reduce the electrical cost. Generally, the thermal efficiency of hydrogen production from water splitting is currently about 50% (1).

Bolton (3) and Bard *et al.* (4) wrote two review articles on solar splitting of water to hydrogen and oxygen in 1996 and 1995, respectively. Although it is very attractive to use two vast resources, water and sunlight, to produce unlimited energy in the form of hydrogen, the efficiency of the conversion of solar energy into chemical energy is estimated to not likely exceed 16% (3).

The different water splitting techniques mentioned above are still under development, except for the electrolysis methods. Although sophisticated large-scale commercial electrolysis units generally have a high electricity-to-hydrogen efficiency of at least 75% (1), electrolysis methods are in industrial use only to a limited extent due to the low overall efficiency of 20–35% (2) and the usually high cost of electrical energy required to operate such units.

Kizling and Järås (5) have recently reviewed applications of plasmas in catalyst preparation and catalytic reactions. Plasmas have been successfully employed to prepare not only dispersions of metal particles on supports but also various support materials, such as silica, alumina, and perovskites. The surface properties of different oxide catalysts can be modified with plasma treatment at low temperatures. These prepared or pretreated catalysts by plasma

[1] To whom correspondence should be addressed.

0021-9517/01 $35.00

methods generally have modified activities and selectivities compared to those by conventional methods. Novel catalytic activities and selectivities for catalytic reactions can also be achieved by the direct application of plasmas to activate reactions, such as nitrogen oxide synthesis, ammonia decomposition or synthesis, and conversion of natural gas into higher hydrocarbons.

Nonequilibrium plasmas have been considered as highly efficient media for use of electrical energy to excite gaseous reactants into highly ionized excited states (the degree of ionization is typically about 10^{-5}). Heating on the order of 10,000 K is required to reach a comparable level of gas excitation by common thermal means. The high energy efficiency in nonequilibrium plasmas can be provided by vibrational excitation of molecules, such as CO, CO_2, N_2, H_2, CH_2, H_2O, and O_2 (6). The vibrational energy accounts for overcoming the activation threshold of endothermic chemical reactions.

Nonequilibrium plasmas have been demonstrated to be effective for methane coupling into higher hydrocarbons, ammonia synthesis from N_2 and H_2, ozone synthesis from air, and the activation of heterogeneous catalysts (7). Rosocha *et al.* have demonstrated that the atmospheric dielectric barrier discharge is a feasible method for destroying halogenated hydrocarbon wastes (8).

Activation of stable abundant molecules, which are very difficult to decompose thermodynamically such as NH_3, H_2S, H_2O, CH_4, and CO_2, is very important in environmental monitoring and protection and vital for exploring their application as raw materials in the areas of synthesis, catalysis, and energy conversion (9). The atmospheric dielectric barrier discharge is ideal for dissociating such stable molecules, as suggested by Eliasson *et al.* (10). Many studies have been done with ammonia (11–13), hydrogen sulfide (13), and methane (14, 15).

Many early studies (from 1900s to 1960s) of water vapor dissociation in electrical discharges at low pressures were carried out with the main purpose of producing free hydroxyl radicals, HO·, and then investigating its chemistry; some had interest in synthesizing hydrogen peroxide (16). Only a few studies on hydrogen production from water splitting with plasmas can be found in the literature.

Antonov *et al.* (17, 18) investigated the mechanisms of dissociation of water molecules for steady-state water vapor discharge at low pressure (0.1–20 Torr). A degree of conversion of initial water molecules of 10–15% has been achieved and a pressure increase in the system is necessary to increase the $(H_2 + O_2)$ output.

Hydrogen production by plasma pyrolysis of water molecules has been evaluated by Srivastava (19) as being technically feasible. The reaction temperature of the process should be around 3400 – 3500 K and the pressure should be 1 atm. The best source for high temperatures would be a plasma jet, which has advantages like instantaneous heating and immediate quenching to avoid a backward reaction of H_2 and O_2 recombination.

Recently, Suib *et al.* (9) have reported the decomposition of CO_2, NO, and H_2O at atmospheric pressure in fan-type ac glow discharge plasmas using plasma and catalyst integrated technologies (PACT) (20). Greater than 60% conversion of H_2O into hydrogen and oxygen can be obtained for H_2O concentration of less than 1.5%.

The H_2 production from water splitting has also been studied with atmospheric dielectric barrier discharges in a tubular PACT reactor in our group (21, 22). The reactor consists of an inner metal-coated electrode that is also a catalyst for the activation of reactants. The atmospheric dielectric barrier discharge between inner and outer electrodes produces a plasma zone for the excitation of molecules. Synergistic effects of catalytic activation and plasma excitation are expected to exist in this tubular reactor.

In this paper, we have more systematically studied the effects of different experimental parameters on the activity for H_2O splitting in the tubular PACT reactors. The experimental parameters are different metal-coated inner electrodes, AC peak voltages applied on the reactors, flow rates of the feed, types and lengths of outer metal electrodes, as well as grounding states of the inner and outer electrodes. Especially, the different types and lengths of outer metal electrodes, as well as grounding states of the inner and outer electrodes, are first discussed in this paper.

2. EXPERIMENTS

2.1. Tubular PACT Reactor

A schematic diagram of a tubular PACT reactor is shown in our previous paper (21). A metal (either Ni, Pd, Rh, or Au) coated (electroless plating, 2 μm thick) copper rod is used as an inner electrode (diameter ϕ: 9.5 mm) and placed in the center of a quartz tube (inner diameter ϕ_{inner}: 9.9 mm; outer diameter ϕ_{outer}: 12.0 mm). Two sets of T-type three way unions at both ends of the quartz tube are used to serve as a reactant inlet and a product outlet, respectively. Two sets of bearings and nuts are employed to keep the inner electrode in the center position of the reactor and to seal the openings between the inner electrode and the unions. The metal-coated inner electrode is believed to act as a catalyst for the activation of reactants. Either Al or Cu foil is wrapped on the outside of the quartz tube to act as an outer electrode. When a high AC voltage (up to 3.0 kV) is applied to both inner and outer electrodes, an atmospheric dielectric barrier discharge is produced between the inner electrode and the part of the quartz tube that is wrapped by the outer electrode. The atmospheric dielectric barrier discharge acts as a plasma to excite molecules carried in through the reactant inlet. Synergistic effects of catalytic

activation and plasma excitation are expected to exist in this reactor.

Tubular PACT reactors with different metal (M) coated inner electrodes (referred as M-tubular PACT reactor) were used to produce H_2 from H_2O splitting at room temperature and atmospheric pressure. Feed compositions were 2.3% of H_2O with a balance of argon and a total flow rate of 10 ml/min. The water concentration was determined from the partial pressure of the water vapor in a bubbler at room temperature assuming that argon is saturated by water vapor after passing through the bubbler. This assumption has been confirmed by measurements of the weight of water collected in a cold trap after the bubbler.

2.2. Circuit for a Tubular PACT Reactor

The circuit diagram for a tubular PACT reactor is also shown in Fig. 1. Reactions are started by initiating a plasma in the tubular PACT reactor. The power to produce the plasma is supplied by a UHV-10 type high frequency (8.1 kHz) AC power supply (made by Nihon Inter Electronics Corporation, Japan). The output voltage of the power supply can be increased directly by increasing its voltage dial setting. The AC voltage waveforms between the inner and outer electrodes in the reactor were recorded with a Yokogawa (Yokogawa Electric Corporation, Japan) DL 1540 digital oscilloscope during reaction via a Tektronix P6025A high voltage probe. The current (I) through the inner and outer electrodes was calculated after measuring the voltage across a standard resistor (100 Ω) with the DL 1540 digital oscilloscope with an Yokogawa 70996 voltage probe.

The typical voltage (V) and current (I) waveforms applied on the tubular PACT reactors are shown in Fig. 2. There is a small phase difference between V and I waveforms. Half of the peak to peak value of the AC voltage waveform and current waveform are defined as the peak voltage (V_p) and peak current (I_p), respectively. V_{rms} and I_{rms} are the root mean square values of V_p and I_p, respectively. The power consumed, P in W or J/s, in the reactor can be obtained using an integration method by taking the time average of

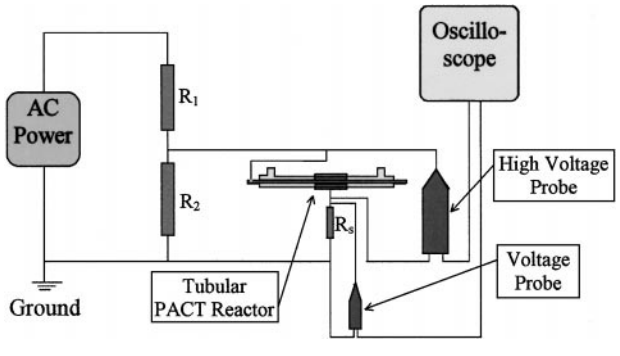

FIG. 1. Circuit diagram for a tubular PACT reactor. R_1, 50 kΩ; R_2, 100 kΩ; R_s, 100 Ω.

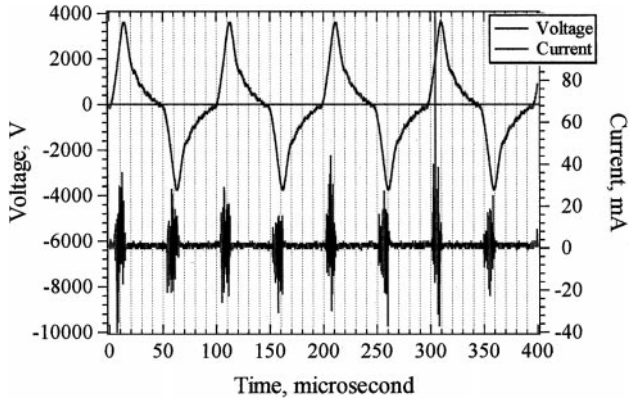

FIG. 2. Typical voltage and current waveforms applied for a tubular PACT reactor.

the integration of the product of V and I recorded in the waveforms, or simply calculated by Eq. [1] when integration is not available:

$$P = 0.64 V_{rms} I_{rms}, \quad [1]$$

where the constant, 0.64, is used to adjust the difference between the result from integration methods and that obtained from the product of V_{rms} and I_{rms} due to the small phase difference between V and I, and is obtained from calibration experiments.

2.3. Product Analysis and Calculations

The outlet gases from the reactor were analyzed on-line with a Hewlett Packard 5890 Series II gas chromatograph (GC) equipped with a Carboxen-1000 (45/60 mesh) column and a thermal conductivity detector. The formation of hydrogen and oxygen in the products was observed with GC methods at levels of 0.2 and 0.1 mol%, respectively.

H_2 yields (Y_H) are calculated from the concentrations of H_2 (C_H) in the product outlet and H_2O (C_W) in the reactant inlet as given in

$$Y_H = (C_H/C_W) \times 100\%. \quad [2]$$

H_2 production rate, R_H, is defined as the number of moles of H_2 produced per unit time (s) in the reactor and calculated according to

$$R_H = QC_w Y_H/(RT), \quad [3]$$

where Q is the feed flow rate of H_2O/Ar in L/s, C_w is the molar concentration of H_2O in the feed, R is the gas constant (0.08206 L · atm/mol · K), and T is room temperature (298 K).

The residence time, t_{res}, of the reactant in the plasma zone with a volume of U in L within the tubular PACT reactors can be calculated by

$$t_{res} = U/Q. \quad [4]$$

TABLE 1

Effects of Different Metal-Coated Inner Electrodes on H_2O Splitting in Tubular PACT Reactors[a]

Coated Metals	V_{rms} $\pm 0.02^b$ (kV)	I_{rms} $\pm 0.2^b$ (mA)	P $\pm 0.05^b$ (W)	C_H $\pm 0.01^b$ (mol%)	Y_H $\pm 0.5^b$ (%)	R_H $\pm 0.1 \times 10^{-8b}$ (mol/s)	E_{eff} $\pm 0.05^b$ (%)
Au	0.33	2.3	0.49	0.18	7.8	1.2×10^{-8}	0.59
Ni	0.33	2.3	0.49	0.16	7.0	1.1×10^{-8}	0.52
Rh	0.33	2.3	0.49	0.13	5.7	9.0×10^{-9}	0.42
Pd	0.33	2.3	0.49	0.11	4.8	7.6×10^{-9}	0.36

[a] Feed: 2.3 mol% H_2O/Ar, 10 ml/min; outer electrode: Al, 6.0 cm, grounded; discharge gap: 0.20 mm.
[b] Standard deviations.

The energy efficiency E_{eff} is defined as the ratio of the theoretical energy required to produce a certain amount of H_2 to the actual energy consumed. E_{eff} is calculated from R_H, P, and the free energy change for water decomposition [$\Delta G^o = 228.74\%\ 10^3$ J/mol at 25°C for $H_2O(g) \rightarrow H_2(g) + 1/2O_2(g)$] (23), as given by

$$E_{eff} = \frac{\text{Theoretical energy required}}{\text{Actual energy consumed}}$$

$$= (R_H \Delta G^o)/P \times 100\%. \quad [5]$$

3. RESULTS

3.1. Effects of Different Metal-Coated Inner Electrodes

The experimental results for H_2O splitting in the tubular PACT reactors with different metal (Au, Ni, Rh, and Pd) coated inner electrodes have been reported in our previous paper (21) and are summarized in Table 1 (see Fig. 3). All experiments were started with fresh metal coated inner electrodes. The experimental results show that the activities for H_2O splitting in the tubular PACT reactors with different metal (Au, Ni, Rh, and Pd) coated inner electrodes are different and decreased in the order

$$\text{Au} > \text{Ni} > \text{Rh} > \text{Pd}.$$

Because all other experimental conditions besides the types of metal coated inner electrode are the same, the energy efficiencies in the tubular PACT reactors with different metal-coated inner electrodes decrease in the same order as above.

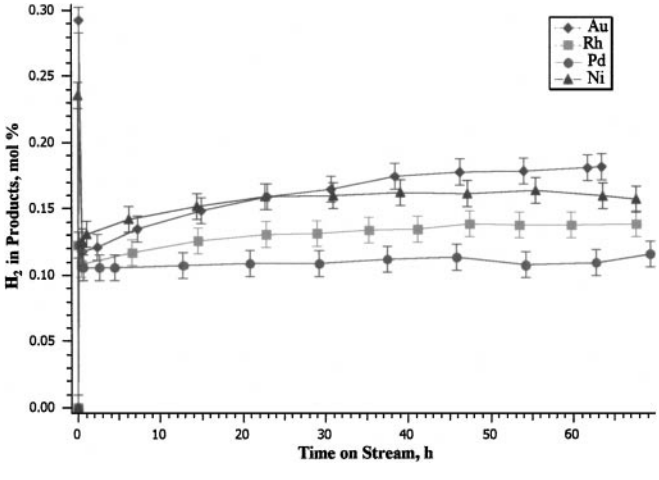

FIG. 3. H_2O splitting in tubular PACT reactors with different metal (Au, Ni, Rh, and Pd) coated inner electrodes (feed: 2.3 mol% H_2O/Ar, 10 ml/min; outer electrode: Al, 6.0 cm, grounded; discharge gap: 0.20 mm).

3.2. Effects of V_p

Effects of different peak voltages on H_2O splitting in tubular PACT reactors were investigated with the reactor with a used Au-coated inner electrode. The results are summarized in Table 2. When V_p increases from 1.2 to 1.8 kV, V_{rms}, I_{rms}, and the power applied to the reactors also increase rapidly. Meanwhile, H_2O splitting activity increases sharply, as shown by the increases in H_2 concentrations in the product, H_2 yield, and H_2 production rates. Meanwhile, the energy efficiency of the reactor achieves a maximum of 0.69% when V_p is 1.4 kV. When V_p was increased further to 3.00 kV, V_{rms}, I_{rms}, and power applied on the reactors also grew gradually, but H_2O splitting activities gradually leveled off. This causes the energy efficiency to drop further. The result achieved here suggests that a certain optimal high V_p is needed to efficiently achieve significant H_2O splitting activity in Au-tubular PACT reactors.

3.3. Effects of Feed Flow Rate

Table 3 gives a summary of effects of feed flow rate Q on H_2O splitting in an Au-tubular PACT reactor. When the feed flow rate increases from 10 to 80 ml/min, the residence time, t_{res}, of 2.3 mol% H_2O/Ar in the plasma zone in the reactor gradually decreases from 2.2 to 0.3 s. The H_2 concentration in the products increases at first from 0.17 mol% at 10 ml/min to 0.22 mol% at 20 ml/min, but decreases gradually to 0.15 mol% at 80 ml/min. The H_2 yield

TABLE 2

Effects of V_p on H_2O Splitting in Au-Tubular PACT Reactor[a]

V_p $\pm 0.02^b$ (kV)	V_{rms} $\pm 0.02^b$ (kV)	I_{rms} $\pm 0.2^b$ (mA)	P $\pm 0.05^b$ (W)	C_H $\pm 0.01^b$ (mol%)	Y_H $\pm 0.5^b$ (%)	R_H $\pm 0.1 \times 10^{-8b}$ (mol/s)	E_{eff} $\pm 0.05^b$ (%)
1.20	0.28	1.8	0.32	0.09	3.8	6.1×10^{-9}	0.43
1.40	0.33	2.3	0.49	0.21	9.2	1.5×10^{-8}	0.69
1.80	0.42	3.2	0.86	0.29	12.7	2.0×10^{-8}	0.54
2.50	0.59	4.2	1.59	0.32	14.0	2.2×10^{-8}	0.32
3.00	0.72	4.8	2.21	0.33	14.2	2.3×10^{-8}	0.23

[a] Feed: 2.3 mol% H_2O/Ar, 10 ml/min; inner electrode: Au; outer electrode: Al, 6.0 cm, grounded; discharge gap: 0.20 mm.
[b] Standard deviations.

shows the same trend as the H_2 concentration. In terms of H_2 production rates, higher feed flow rates offer higher H_2 production rates. When the feed flow rate increases and all other experimental parameters are the same, V_{rms}, I_{rms}, and power applied to the reactors do not change. The energy efficiencies in the tubular PACT reactors increase with the increasing feed flow rates. This suggests that high feed flow rates are preferred in terms of energy efficiency and H_2 production rate.

3.4. *Effects of Different Lengths of Al Outer Electrode*

Table 4 gives a summary of effects of different lengths of Al outer electrode on H_2O splitting in an Au-tubular PACT reactor. When the length increases from 2.0 to 8.0 cm, the residence time of 2.3 mol% H_2O/Ar in the plasma zone in the reactor linearly grows from 0.7 to 2.9 s. Meanwhile, the H_2 concentration in the products at first increases from 0.17 mol% at 2 cm to 0.23 mol% at 4.0 cm and levels off until 8.0 cm. The H_2 yield and H_2 production rate show the same trend as the H_2 concentration. I_{rms} and P increase linearly with increasing length of outer Al electrodes when V_p and V_{rms} are kept the same. Because the variation of H_2O splitting activity is much less than the change of the power applied to the reactors, energy efficiency decreased almost linearly with increasing length. This suggests that the length of the Al outer electrode has a significant effect on the energy efficiency for H_2O splitting activity in tubular PACT reactors and should be optimized in order to achieve both high H_2O splitting activity and high energy efficiency (see also Fig. 4).

3.5. *Effects of Different Outer Electrodes*

Different outer electrodes (Al or Cu foils) were used to investigate their effects on H_2O splitting in tubular PACT reactors and the results are shown in Table 5. No significant activity difference was observed for H_2O splitting in Au-tubular PACT reactors with different outer electrodes.

3.6. *Effects of Grounding Inner or Outer Electrodes*

For safety reasons, the circuit for the tubular PACT reactors should be connected to ground at a certain point. No significant activity difference was observed for H_2O splitting in Au-tubular PACT reactors when the grounding was

TABLE 3

Effects of Feed Flow Rate Q on H_2O Splitting in Au-Tubular PACT Reactor[a]

Q $\pm 1^b$ (ml/min)	t_{res} $\pm 0.1^b$ (s)	V_{rms} $\pm 0.02^b$ (kV)	I_{rms} $\pm 0.2^b$ (mA)	P $\pm 0.05^b$ (W)	C_H $\pm 0.01^b$ (mol %)	Y_H $\pm 0.5^b$ (%)	R_H $\pm 0.1 \times 10^{-8b}$ (mol/s)	E_{eff} $\pm 0.05^b$ (%)
10	2.2	0.43	3.4	0.94	0.17	7.2	1.1×10^{-8}	0.28
20	1.1	0.43	3.4	0.94	0.22	9.4	3.0×10^{-8}	0.73
30	0.7	0.43	3.4	0.94	0.21	9.1	4.4×10^{-8}	1.06
40	0.5	0.43	3.4	0.94	0.19	8.3	5.3×10^{-8}	1.29
60	0.4	0.43	3.4	0.94	0.18	7.7	7.4×10^{-8}	1.80
80	0.3	0.43	3.4	0.94	0.15	6.7	8.5×10^{-8}	2.09

[a] Feed: 2.3 mol% H_2O/Ar; inner electrode: Au; outer electrode: Al, 6.0 cm, grounded; discharge gap: 0.20 mm; V_p: 1.80 kV.
[b] Standard deviations.

TABLE 4

Effects of Different Lengths of Al Outer Electrode on H_2O Splitting in Au-Tubular PACT Reactor[a]

Length ±0.1[b] (cm)	t_{res} ±0.1[b] (s)	V_{rms} ±0.02[b] (kV)	I_{rms} ±0.2[b] (mA)	P ±0.05[b] (W)	C_H ±0.01[b] (mol%)	Y_H ±0.5[b] (%)	R_H ±0.1 × 10^{-8}[b] (mol/s)	E_{eff} ±0.05[b] (%)
2.0	0.7	0.32	1.3	0.27	0.17	7.7	1.2×10^{-8}	1.05
4.0	1.5	0.32	2.0	0.41	0.23	10.1	1.6×10^{-8}	0.90
6.0	2.2	0.32	2.4	0.49	0.24	10.5	1.7×10^{-8}	0.78
8.0	2.9	0.32	3.1	0.63	0.22	9.8	1.6×10^{-8}	0.56

[a] Feed: 2.3 mol% H_2O/Ar, 10 ml/min; inner electrode: Au; outer electrode: Al, grounded; discharge gap: 0.20 mm; V_p: 1.40 kV.
[b] Standard deviations.

switched between the inner Au electrode and Al outer electrode, as shown in Table 6.

4. DISCUSSION

4.1. Effects of Different Metal Coated Inner Electrodes

The activities of water splitting in the tubular PACT reactors with different metal-coated inner electrodes (thereafter referred as metal reactors) are significantly different, as shown in Table 1. Table 7 summarizes the activities and some electrical properties of the coated metals. No direct relationship can be found between the activities and either the resistivities or work functions of the coated metals, suggesting that some chemical properties, possibly catalytic effect, of coated metals may play important roles in H_2O splitting in tubular PACT reactors. Furthermore, when compared to a tubular plasma reactor with a nonmetallic (quartz) inner electrode with similar dimensions (thereafter referred as all quartz reactor), the H_2 yields are much higher in the metal reactors, indicating the catalytic effect of metal coated inner electrodes on the reaction (22).

Argon is the main component of the feed to tubular PACT reactors and is excited initially in the plasma zone, as evidenced by OES (optical emission spectroscopy) studies (22). The OES studies also reveal that emission intensities of all excited Ar* species in the plasma zone decrease in different proportions after H_2O is introduced into the system. This suggests that excited argon species will selectively transfer their energy to the introduced water molecules and excite them into excited states, H_2O^*, as evidenced by the detection of hydroxyl radicals in H_2O/Ar plasmas. The probability that water molecules are excited directly in the plasma zone is much smaller due to the much lower population of water molecules. The possible reaction mechanism for H_2O splitting in the plasma zone can be proposed as

$$H_2O + Ar^* \leftrightarrow H_2O^* + Ar \quad [6]$$

$$H_2O^* \leftrightarrow HO\cdot + H\cdot \quad [7]$$

$$HO\cdot + Ar^* \leftrightarrow H\cdot + O\cdot + Ar \quad [8]$$

$$2H\cdot \leftrightarrow H_2 \quad [9]$$

$$2O\cdot \leftrightarrow O_2. \quad [10]$$

The excited water molecules in metal reactors can be adsorbed on the metal surfaces and involved in catalytic dissociation reactions, leading to dissociation into hydrogen

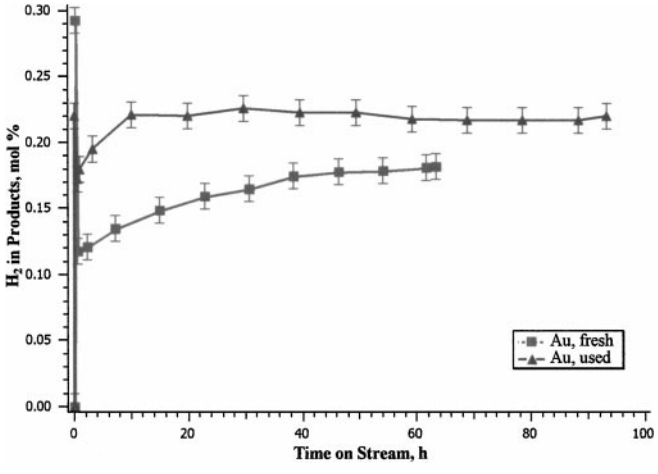

FIG. 4. H_2O splitting in tubular PACT reactors with fresh and used Au-coated inner electrodes (feed: 2.3 mol% H_2O/Ar, 10 ml/min; outer electrode: Al, 6.0 cm, grounded; discharge gap: 0.20 mm).

TABLE 5

Effects of Different Outer Electrodes on H_2O Splitting in Au-Tubular PACT Reactor[a]

Outer electrode	H_2 in products (±0.01[b], mol%)	H_2 yield (±0.5[b], %)
Al	0.24	10.4
Cu	0.23	9.8

[a] Feed: 2.3 mol% H_2O/Ar, 10 ml/min; inner electrode: Au; outer electrode: 6.0 cm, grounded; discharge gap: 0.20 mm; V_p: 1.80 kV.
[b] Standard deviations.

TABLE 6

Effects of Grounding Inner or Outer Electrodes on H_2O Splitting in Au-Tubular PACT Reactor[a]

Grounded electrode	H_2 in products ($\pm 0.01^b$, mol%)	H_2 yield ($\pm 0.2^b$, %)
Outer Al electrode	0.20	8.5
Inner Au electrode	0.21	8.9

[a] Feed: 2.3 mol% H_2O/Ar, 10 ml/min; inner electrode: Au; outer electrode: 6.0 cm; discharge gap: 0.20 mm; V_p: 1.80 kV.
[b] Standard deviations.

and oxygen atoms which then form hydrogen and oxygen molecules. Especially, oxygen radicals (O·) will be adsorbed on metal surfaces and ether combined into O_2 or react with the metal surfaces, and therefore shift the equilibrium of water splitting toward the decomposition of H_2O and producing H_2 with high yields, even higher than that predicted by thermodynamics. This is supported by the absence of O· and much lower concentration of HO· with metal reactors. In the case of all quartz reactors, interactions between the quartz surface and O· are not observed and some homogeneous reactions in the plasma zone, such as reactions 7 and 8, are probably governed by thermodynamic equilibria, as evidenced by the OES studies (22). This explains the much lower H_2 yield in the all quartz reactor with respect to the metal reactors.

4.2. *Effects of V_p*

When V_p applied across the inner and outer electrodes of an Au-tubular PACT reactor increases, the power applied in the reactor and H_2O splitting activities jump quickly at low values of V_p (1.2 to 1.8 kV), as shown in Table 2. When V_p is further increased to 3.0 kV, which is the highest V_p that can be reached with the UHV-10 power supply in this research, the H_2O splitting activities gradually level off while the applied power continuously grows. The energy efficiency jumps sharply at low V_p (1.2 to 1.4 kV) and achieves a maximum of 0.72% when V_p is 1.4 kV, but gradually decreases at higher V_p values.

When V_p increases, higher excitation temperatures in the plasma zone can be achieved. Therefore, more excited species are populated at higher energy levels, as evidenced by the increasing intensities of emission lines with increasing V_p for plasmas of pure carrier gases (such as Ar, He, and N_2) (22). The efficiency for the energy transfer from excited carrier gas species to reactant molecules generally increases with increasing V_p, as concluded by Luo and coworkers from their OES studies using the tubular PACT reactor system (22). This may explain the effects of V_p on the activity of H_2O splitting in Au-tubular reactor.

On the other hand, the quartz tube in the tubular PACT reactors in the circuit can be considered as a combination of a capacitor and a resistor in parallel with each other (24). The decreasing energy efficiency at high V_p may be due to most of the increasing energy being consumed to overcome the increased resistance and impedance of the reactor due to higher temperature of the reactor at high V_p. This may explain the leveling off behavior of H_2O splitting activities at very high V_p values (>2.5 kV).

TABLE 7

H_2O Splitting Activity in Tubular PACT Reactors with Different Metal-Coated Inner Electrodes and Some Electrical Properties of Coated Metals

Metal	H_2 in products, ($\pm 0.01^b$, mol%)	Resistivity[a] at 20°C ($\mu\Omega \cdot$ cm)	Work function[a] (eV)
Au	0.18	2.24	5.1
Ni	0.16	6.84	5.15
Rh	0.13	4.51	4.98
Pd	0.11	10.54	5.12

[a] From Ref. (23).
[b] Standard deviations.

4.3. *Effects of Feed Flow Rate*

Although there is an optimum range of feed flow rates (about 20–30 ml/min) in terms of high H_2 yields, the variations of H_2 yields are small and the highest Y_H is only about 40% higher than the lowest Y_H, as shown in Table 3. The increased H_2 production rate mainly contributed by the increasing of the feed flow rate is much more distinct than the variations of H_2 yields. When the feed flow rate increases 8 times from 10 to 80 ml/min, R_H increases almost proportionally with the feed flow rate and also grows 8 times from 1.1×10^{-8} to 8.5×10^{-8} mol/s. The energy efficiency also increases almost proportionally with the increasing of the feed flow rate because the higher H_2 production rates are achieved with higher feed flow rates while the power consumed in the reactors is the same for different feed flow rates. In summary, high feed flow rates are preferred in terms of achieving high H_2 production rate and reactor efficiency.

The existence of an optimum range of feed flow rates (about 20–30 ml/min) in terms of high H_2 yields reflects that an optimum range of residence times (0.7–1.1 s) for reactants in the plasma zone within the reactor is needed to achieve optimum H_2 yields. H_2O may not achieve optimum excitation in the plasma zone with a short t_{res} and cannot be further dissociated into H_2 and O_2. On the other hand, reverse H_2O formation from H_2 and O_2 is more probable when a long t_{res} is employed.

4.4. *Effects of Different Lengths of Al Outer Electrode*

The residence times of 2.3% H_2O/Ar in the plasma zone within the tubular PACT reactors become proportionally

longer with increasing length of the outer electrode at a fixed feed flow rate of 10 ml/min, as shown in Table 4. The dependence of H_2 yields on t_{res} has shown the same trend as in the case of changing feed flow rates while keeping the outer electrode at the same length. In other words, an optimum range of lengths of the outer electrode and therefore ideal t_{res} are needed to achieve high H_2 yields.

Although there is an optimum length (about 4.0 to 6.0 cm) for the outer electrode in terms of high H_2O splitting activities, the variations of H_2O splitting activities are smaller compared to the change of energy efficiencies, as shown in Table 4. When the length of outer electrodes increases, the capacitance and the resistance or impedance of the reactor will increase. The observed decreasing energy efficiency at a longer length of outer electrodes may be due to energy consumption in order to overcome increases in the capacitance and resistance or impedance instead of using the energy in H_2O splitting.

4.5. Effects of Different Outer Electrodes

No significant activity difference was observed for H_2O splitting in Au-tubular PACT reactors with different outer electrodes (Al or Cu foils), as shown in Table 5. This may be due to the fact that there is no catalytic effect from outer metal electrodes because there is no direct contact of reactants with outer electrodes.

4.6. Effects of Grounding Inner or Outer Electrodes

No significant activity difference was observed for H_2O splitting in Au-tubular PACT reactors when the grounding was switched between the inner Au electrode and outer Al electrode, as shown in Table 6. This may be because it does not change the plasma in the reactor and because of the catalytic effect of inner Au-coated electrode when the grounding state was switched.

5. CONCLUSIONS

In this research, significant hydrogen production (0.33 mol% in products) from H_2O splitting by atmospheric dielectric barrier discharges has been achieved with tubular plasma reactors at room temperature. The effects of different metal (either Ni, Pd, Rh, or Au) coated inner electrodes, type and length of outer metal (either Al or Cu) electrodes, grounding state of the inner and outer electrodes, AC peak voltages applied on the reactor, and the flow rate of the feed (2.3 mol% in He) have been systematically studied. The water-splitting activity and its energy efficiency vary with the type of metal-coated inner electrodes, peak voltage, the length of outer electrode, and feed flow rate, but they do not depend on the type of outer metal electrodes and the grounding state of inner and outer electrodes. In order to understand the observed phenomena of water splitting in the tubular PACT reactors, more detailed OES diagnostic studies of plasma chemistry and surface characterization of used metal coated inner electrodes are needed and currently in progress.

H_2O splitting in tubular plasma reactors in this research has advantages over other processes in that it is a simple process which occurs at room temperature and atmospheric pressure. However, the energy efficiency for this process is generally still low (<3%). There are still other variables that can be optimized to further improve the efficiency of this process. These variables include high flow rates, high water concentrations, and different carrier gases. The circuit design and power supply frequency are other variables that can influence the energy efficiency for the reaction.

REFERENCES

1. Thomas, N. C., *Sci. Prog.* **72**, 32 (1988).
2. Czuppon, T. A., Knez, S. A., and Newsome, D. S., *in* "Encyclopedia of Chemical Technology," 4th ed. (Kirk-Othmer, Ed.), Vol. 13, p. 867. Wiley, New York, 1991.
3. Bolton, J. R., *Solar Energy* **57**, 37 (1996).
4. Bard, A. J., and Fox, M. A., *Acc. Chem. Res.* **28**, 141 (1995).
5. Kizling, M. B., and Järås, S. G., *Appl. Catal. A: General* **147**, 1 (1996).
6. Fridman, A. A., and Rusanov, V. D., *Pure Appl. Chem.* **66**, 1267 (1994).
7. Badyal, J. P. S., *Top. Catal.* **3**, 255 (1996).
8. Rosocha, L. A., *et al.*, *in* "Non-Thermal Plasma Techniques for Pollution Control" (B. M. Penetrante, and S. E. Schultheis, Eds.), Vol. G 34, Part B, p. 281. Springer-Verlag, Berlin, 1993.
9. Suib, S. L., Brock, S. L., Marquez, M., Luo, J., Matsumoto, H., and Hayashi, Y., *J. Phys. Chem. B* **102**, (1998).
10. Eliasson, B., Egli, W., and Kogelschatz, U., *Pure Appl. Chem.* **66**, 1275 (1994).
11. Miller, G. P., and Baird, J. K., *J. Phys. Chem.* **97**, 10,984 (1993).
12. Venugopalan, M., and Veprek, S., *in* "Plasma Chemistry IV" (S. Veprek and M. Venugopalan, Eds.), Vol. 107, p. 9. Springer-Verlag, Berlin, 1983.
13. Chang, M. B., and Tseng, T. D., *J. Environ. Eng.* **122**, 41 (1996).
14. Huang, J., and Suib, S. L., *J. Phys. Chem.* **97**, 9403 (1993).
15. Suib, S. L., and Zerger, R. P., *J. Catal.* **139**, 383 (1993).
16. Venugopalan, M., and Jones, R. A., "Chemistry of Dissociated Water Vapor and Related System." Interscience, New York, 1968.
17. Antonov, E. E., Dresvyannikov, V. G., and Popovich, V. I. *J. NewEnergy* **1**, 6 (1996).
18. Antonov, E. E., Dresvyannikov, V. G., and Popovich, V. I., *J. New Energy* **1**, 69 (1996).
19. Srivastava, S. K., *Fuel Sci. Technol.* **14**, 39 (1995).
20. Hayashi, Y., and Wakatsuki, N., U.S. Patent 5,474,747, 1995.
21. Chen, X., Marquez, M., Rozak, J., Marun, C., Luo, J., Suib, S. L., Hayashi, Y., and Matsumoto, H., *J. Catal.* **178**, 372 (1998).
22. Luo, J., Suib, S. L., Hayashi, Y., and Matsumoto, H., *J. Phys. Chem. A* **103**, 6151 (1999).
23. Weast, R. C., "CRC Handbook of Chemistry and Physics," 67th ed. CRC Press, Boca Raton, FL, 1986.
24. Wang, J.-Y., Xia, G.-G., Huang, A., Suib, S. L., Hayashi, Y., and Matsumoto, H., *J. Catal.* **185**, 152 (1999).